Proceedings of the
47th IEEE Conference on Decision and Control
Cancun, Mexico, Dec. 9-11, 2008

Dynamic Calibration of Adaptive Optics Systems: A System Identification Approach

Alessandro Chiuso, Riccardo Muradore and Enrico Marchetti

Abstract— **Adaptive optics is used in astronomy to obtain high resolution images, close to diffraction limited, of stars and galaxies with ground telescopes, otherwise blurred by atmospheric turbulence. The measurements of one or more wavefront sensor are used to flatten distorted wavefronts with one or more deformable mirror in a feedback loop. In this paper we shall report our experience on the problem of building an accurate (dynamical) model of the actuation (deformable mirror) and sensing (wavefront sensor) of adaptive optics system. This will be done adapting state-of-the-art system identification and model reduction techniques to the problem at hand. Our results are based on *real* data collected under various operating conditions from a demonstrator developed at the European Southern Observatory (ESO), which is now operating in the Paranal observatory (Chile).**

Index Terms— **Adaptive Optics, Closed Loop Identification, Subspace Methods.**

I. Introduction

Adaptive optics (AO) is a recent engineering discipline arising from the interconnection of optics, electro-optics, electrical engineering, mechanical engineering and chemistry, [26].

In order to provide diffraction limited performance, rivalling that obtained from the Hubble Space Telescope, with ground-based telescopes, AO techniques use the measurements of one or more wavefront sensor (WFS) to flatten distorted wavefronts with one or more deformable mirror (DM, from a control point of view the "actuator") in a feedback loop [25], [26], [11]. The cascade of these two components (DM + WFS) represents what in this paper will be called the *plant* or *system*.

In this paper we shall work with an adaptive optics system called Multi-Conjugate Adaptive Optics Demonstrator (MAD) [20], which is a demonstrator instrument aiming at performing large field of view atmospheric turbulence correction by implementing for the first time an adaptive optics technique called Multi-Conjugate Adaptive Optics (MCAO). MCAO and similar atmospheric turbulence correction techniques have been recognized as strategic both for the 2nd generation Very Large Telescope (VLT) instrumentation and for the European Extremely Large Telescope (E-ELT).

State-of-the-art systems, such as MAD considered in this paper, are based on a very simple static approximation of the system. Section IV contains a brief description of how this problem is currently tackled. The main motivation for using such a simple approximation of the plant is that the frequency response of the actuators is essentially constant in the frequency band of interest and that, by physical considerations, the wavefront sensor can be modeled as an averaging block on a sampling interval.

Further considerations concerning modeling of an adaptive optics system can also be found in [18], [19], [23] where an optimal (minimum variance or LQG) approach to control design is taken. In any case the models considered, besides their static gain, are always based on physical considerations and are not built starting from data. Model based control techniques have also been put forward in [15], [13]; these works can be thought of as being complementary to our work.

In this paper we shall report our experience on the problem of building an accurate (dynamical) model of (the deterministic part of) an Adaptive Optics system. Our results are based on real data collected under various operating conditions from MAD. Data have been collected when MAD was sitting at the ESO facilities in Garching, before being shipped to the Paranal observatory (Chile) for the actual test on the field.

In our view, the main contribution of this paper is to show that, indeed, a well designed dynamical model can outperform (in the sense of improving of about one order of magnitude in terms of simulation error variance) state-of-the-art static models which are now being used for control design. We also expect that the same consideration will become more and more important in the future; in fact, the next generation's AO systems will most likely have a control loop operating at higher frequency, making it even less reasonable to model the system with a static gain.

The models have been obtained using very recently developed subspace techniques [7], which have also allowed identification to be performed in closed loop, and hence around the nominal operating conditions. As a side contribution, we have also implemented a recursive version (see Section V-A) of the PBSID$_{opt}$ algorithm in [7], which has allowed to handle the large data sets used in this paper. Finally, model reduction techniques have been applied to the models obtained from the identification experiment, allowing to obtain reasonably sized models, while maintaining good

A. Chiuso is with the Dipartimento di Tecnica e Gestione dei Sistemi Industriali, Università di Padova (sede di Vicenza), stradella San Nicola, 3 - 36100 Vicenza, Italy. E-mail: chiuso@dei.unipd.it. The work of this author is partially supported by the national project *New techniques and applications of identification and adaptive control* funded by MIUR

R. Muradore is now with the Department of Computer Science, University of Verona, Strada Le Grazie 15, Ca Vignal 2, 37134 Verona (ITALY); part of this work was performed while he was with European Southern Observatory, Garching bei München, Germany. riccardo.muradore@univr.it

E. Marchetti is with the European Southern Observatory, Garching bei München, Germany. emarchet@eso.org

performance in validation.

II. Adaptive Optics: SCAO vs. MCAO

In the so called *single conjugated adaptive optics* (SCAO) systems the wavefront distortion is measured by one wavefront sensor (see Section III). These measurements are used to control one deformable mirror (see Section III) which is used to compensate for the phase delays.

The field of view which benefits from the real-time atmospheric turbulence correction is very limited, typically few arcseconds for images obtained at infrared wavelengths. This limitation is coming from the fact that the distorted wavefront is estimated by the wavefront sensor only in the direction of a sufficiently bright guide star located at or nearby the observed astronomical object, and it is corrected for the same direction by a deformable mirror.

In this configuration only the volume of the atmosphere probed by the light of the observed guide star is efficiently sensed while the atmospheric volumes probed by astronomical objects far from the guide star are only partially seen. This phenomenon is called atmospheric anisoplanatism and a graphical representation is given in Figure 1.

To overcome these inconveniences, systems based on the so called *Multi-Conjugate Adaptive Optics* are being built. This technology allows to correct for atmospheric turbulence on a field of view which is much larger than the one typically covered by the existing adaptive optics systems installed on 8-meter class telescopes. The principle behind MCAO is described pictorially in Figure 1. MCAO senses and corrects for the whole atmospheric volume probed by the observed field of view, [24].

ESO has developed a Multi-Conjugate Adaptive Optics Demonstrator (MAD) which, after a long period of testing at the ESO premises, has been installed on a Very Large Telescope (VLT) in the Paranal observatory on early 2007 for evaluating its correction performance.

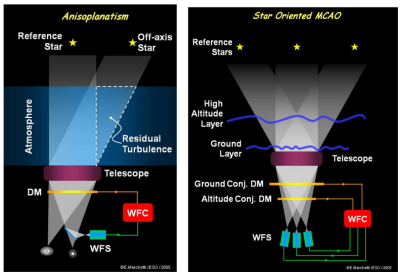

Fig. 1. Left to right: SCAO with atmospheric anisoplanatism, MCAO.

MAD is a MCAO systems with 2 deformable mirrors (bimorph mirror, 60 elements), [2]. The system is equipped with Multi Shack-Hartmann WFS consisting of 3 Shack-Hartmann units (SHU).

III. Plant description: Deformable Mirrors and Wavefront Sensors

This section is dedicated to the description of the main components of an AO system: the deformable mirror and the wavefront sensor. In this paper, indeed, we are interested in providing a mathematical description of how voltages applied to the deformable mirror map to sensed wavefront gradients.

The deformable mirrors of MAD are made of two piezoelectric ceramic wafers, bonded together and oppositely polarized. An array of electrodes is deposited between the two wafers, while the front and back surfaces are grounded. When a voltage is applied to an electrode, one wafer contracts locally while the other expands creating a bend. To ensure the maximum mobility to the DM, it is only fixed on a tip/tilt mount with three support points, located at the edge of the mirror and equally spaced. The layout of the actuators is sketched in figure 2 (left panel). The piezo actuators have several resonances in high frequency which influence their dynamic behavior also in the closed-loop bandwidth. This mirror is also affected by hysteresis. Fortunately when the system is working in closed loop, this nonlinear effect does not have a strong impact.

The second fundamental component of any AO system is the wavefront sensor. This is the device that measures how far the corrected wavefront is with respect to the ideal (no atmospheric turbulence or perfect correction) flat wavefront. In the MAD project the sensor is a Multi Shack-Hartmann WFS consisting of 3 Shack-Hartmann units (SHU). Each SH sensor provides the gradients of the 2D shape of the wavefront in a number of points along a cartesian pattern. The main components of the SH sensor are a lenslet array located in a conjugated pupil plane and an array of detectors placed in the focal plane of each lens (see figure 2, right panel). The incoming wavefront is spatially sampled by the lenslet and each subaperture focuses the incident light in the focal plane. If the wavefront is flat the intensity distribution is, as a function of wavelength λ, the Fourier transform of the subaperture; for a tilted wave the intensity distribution is shifted and possibly blurred. x and y slopes are reconstructed from the shift.

IV. Control aspects

For ease of exposition, we will consider a SCAO system schematically described in figure 2. The control loop is composed by one WFS and one DM. The same procedure can be extended to the more general MCAO case, involving several WFSs and several DMs. In this simplified scheme we shall only consider the piezoelectric part of the mirror and assume orientation/tip/tilt have been taken care of.

The symbols in figure 2 have the following meaning: $\mathbf{w}$ is the incoming turbulence, $\mathbf{c}$ is the DM correction, $\tilde{\mathbf{w}}$ is the residual error, $\mathbf{y}$ is the measurement vector (sensed slopes) and $\mathbf{n}$ is the measurement noise. The signal $\mathbf{u}$ is the control input (i.e. the voltages applied to the DM) and $\mathbf{d}$ is an excitation source which is normally zero and has been added only to the purpose of identification, see Section V.

The signals $\mathbf{y}$, $\mathbf{u}$ and $\mathbf{n}$ are discrete-time finite-dimensional vectors. The dimension of $\mathbf{y} \in \mathbb{R}^p$ is twice the number of illuminated subapertures on which the incoming turbulence is spatially sampled. The dimension of $\mathbf{u} \in \mathbb{R}^m$ is equal to the number of actuators of the deformable mirror. On the

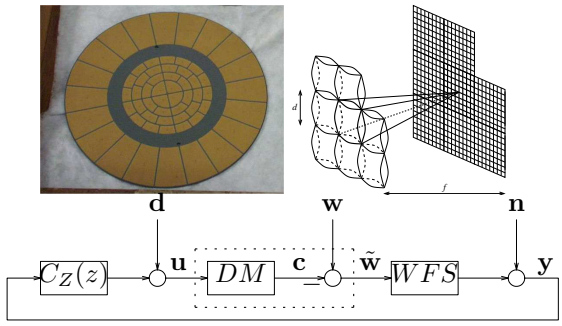

Fig. 2. Top left: deformable mirror. Top right: wavefront sensor principle. Bottom: Adaptive optics block diagram.

other hand, the quantities $\mathbf{w}$, $\mathbf{c}$ and $\tilde{\mathbf{w}}$ are continuous signals in time and space, with a finite spatial support equal to the pupil size[1]. The objective of the controller is to produce an input $\mathbf{u}$ such that the mirror compensates for the measured residual error $\mathbf{y}$. Since the DM + WFS system is usually modeled as a static mapping M_I, i.e. $\mathbf{y} \simeq M_I \mathbf{u}$, the desired inputs $\mathbf{u}$ are of the form $M_C \mathbf{y}$ where the so-called control matrix M_C is simply obtained by pseudo-inverting the so-called interaction matrix M_I. These reference signals are fed into a linear controller, which is usually composed by m PI controllers of the form $C_{PI}(z) = K_p + K_i \frac{T_s}{1-z^{-1}}$. Therefore $C_Z(z)$ in Figure 2 takes the form

$$C_Z(z) = \mathsf{diag}\left\{C_{PI}(z), \ldots, C_{PI}(z)\right\} M_C \tag{1}$$

Since the control matrix M_C is used to reconstruct the required DM pattern at the next step from the current WFS measurements, the performance of the controller (1) is strictly related to the *quality* of M_C and hence to that of M_I. Finding the matrix M_I is normally called *calibration*. This problem can be tackled in a number of ways, see [22], [17]. The most commonly used procedure (and the one implemented in MAD) is based on exciting the mirror with a sequence of inputs which are orthogonal to each other; the input pattern is based on the so-called Hadamard matrix. The constant input is applied as long as the system reaches steady state. The (temporal) average of the steady state response is taken as output.

The results of this paper provide an alternative procedure for calibration. In fact, once a dynamical model relating control inputs $\mathbf{u}$ to outputs $\mathbf{y}$ has been obtained via system identification, a static approximation can be found by, e.g. considering the DC gain of the identified model. Of course the static approximation can be seen as the zero-order approximation of the identified model. We shall discuss in Section V-B the application of model reduction techniques to this problem; the results are quite interesting, see Section VI.

Note that the dynamic model derived here could be integrated with the data-driven model for the turbulence in [15], as an input to a model-model based control design technique where, instead, the standard static modeling approach of the deterministic part (WFS + DM) has been used (the interaction matrix is called H there, see eq. (30) and Corollary 1 in [15]).

[1]For easy of exposition signal conversion (continuous to discrete time and viceversa) are not explicitly shown in Figure 2.

V. Identification

In this paper we address, for the Multi-Conjugate adaptive optics system, the identification of a dynamical model linking the control action to *one* DM to the slope measurements of *one* WFS. The disturbance $\mathbf{d}$ in Figure 2 has to be injected in order to guarantee identifiability. During normal operation of the plant $\mathbf{d} = 0$. It is therefore advisable to keep $\mathbf{d}$ as small as possible also during identification in order to operate the plant around the nominal working conditions.

We shall get back to this point when discussing the experimental results. Suffices here to say that the results from validation experiments on the real plant suggest that $\mathbf{d}$ should be large enough to excite the systems and small enough not to excite non-linear effects.

One might wonder why one should dare to perform identification in closed loop; the most important reason is the non-linearity of the system. In fact, the overall plant can be considered linear only in the vicinity of the operating conditions; in particular the wavefront sensor should not saturate i.e. the sensed slope should be small; this can only be achieved in closed loop.

To these considerations we might also add that, under constraints on the input spectrum and/or on the model structure, sometimes closed-loop identification gives better results than open-loop [4] as far as identification of the "deterministic part" (the one we are interested in); note also it could be desirable to perform identification in closed-loop when the model have to be used for the purpose of control design [12], [16]. We shall not further elaborate on this issue and, for reason of space, we refer the reader to the above referenced papers.

The system is MIMO with 60 inputs and 104 outputs; therefore it is quite natural to use a subspace approach. Our aim here is not to provide an in-depth comparison of subspace methods applied to the AO system, but rather show that these methods provide an interesting alternative to the most commonly used calibration procedures [17] which are being normally used in the AO community. Note, incidentally, that the recent works [15], [13] consider data-driven control strategies which concentrate on the "stochastic" part, i.e. the atmospheric turbulence, while still using the standard static model (interaction matrix) for the "deterministic" part of the system (DM + WFS).

The main issue, besides the presence of feedback, is the large number of inputs (60) and outputs (104); to the authors' knowledge the PBDSI$_{opt}$ algorithm described in [7], [6] is the simplest (in terms of computational load) subspace algorithm consistent with closed-loop data. It turns out that the results in [7], [6] imply also that PBDSI$_{opt}$ is (asymptotically) optimal within a certain class of subspace algorithms.

Moreover, in order to deal with the large amount of data we have implemented a recursive version of the algorithm which is based on the recursive computation of the VARX[2] parameters. In the next subsection we give an outline of the algorithm; we refer the reader to the papers [3], [7], [6] for a thorough discussion of the literature on subspace methods as well as for the properties of the PBSID$_{opt}$ algorithm.

Our purpose is to estimate the parameters (A, B, C, K) of the innovation state space model

$$\begin{aligned} \mathbf{x}(t+1) &= A\mathbf{x}(t) + B\mathbf{u}(t) + K\mathbf{e}(t) \\ \mathbf{y}(t) &= C\mathbf{x}(t) + \mathbf{e}(t) \end{aligned} \tag{2}$$

where $\mathbf{e}(t)$ is the one step-ahead linear prediction error of $\mathbf{y}(t)$ given $\{\mathbf{y}(s), \mathbf{u}(s), s < t\}$. Note also that we assume there is a delay between inputs and outputs; this is reasonable for this application.

We shall also denote with $F(z) := C(zI - A)^{-1}B$ the transfer function from $\mathbf{u}$ (control inputs) to $\mathbf{y}$ (sensed slopes). This is precisely the model for the "deterministic" system (DM + WFS) we seek for. The "stochastic" part $G(z)\mathbf{e} := \left(C(zI - A)^{-1}K + I\right)\mathbf{e}(t)$ models the contribution of the measurements noise $\mathbf{n}$ (see Fig. 2). Note that in our identification setup (calibration on beacon) the wavefront phase variation due to atmospheric turbulence is zero, i.e. $\mathbf{w} = 0$.

In subspace identification two integers, p for "past" and f for "future", have to be selected by the user. These are the number of block rows in certain block Hankel data matrices we shall encounter later on. The choice of these parameters is not entirely trivial, and in fact this is subject of current research [3], [7]. In Section VI we shall briefly discuss these choices.

A. Recursive Implementation

In the application we are considering handling large data sets is quite demanding as both computation and memory requirements are concerned. Therefore we have implemented a recursive estimator for the VARX coefficients in the PBSID$_{opt}$ algorithm based on the recursive least squares algorithm [27]. The same algorithm had been used in [8].

In order to provide a fully recursive implementation of the PBSID$_{opt}$ algorithm, besides using RLS in the VARX estimation step, it is also necessary to implement both (i) the SVD and (ii) the estimation of A, B, C, K from the state sequences in a recursive manner.

As far as the SVD step, there are a number of techniques for updating the SVD when more data points become available. This includes rank-1 updates [5] and subspace tracking techniques [9], [14], [29].

B. Reduced Order Models

As can be seen from the results reported in Section VI, in order to obtain good performance, the identified model order should be in the range $[100, 140]$. It turns out that this is a rather large model which might impose limitations to the purpose of control design. Therefore we have explored the possibility of using reduced order models.

In this paper we consider the balanced model reduction. However standard balanced model reduction does not preserve the DC-gain of the system, which, as we have seen in the previous sections, plays a crucial role in this application. Therefore we shall consider a procedure which preserves the DC gain, called *DC-preserving balanced model reduction* [1], also known as *singular perturbation approximation*.

VI. Results

We have carried out identification and validation experiments using *real data* operating the system in closed-loop, under the so-called *calibration on beacon* setup, i.e. when the mirror is illuminated with a constant light (no incoming atmospheric aberrations). The controller used to close the loop is the same for all data records.

The identification was carried out using $\bar{N} = 40000$ data points. The length of the past horizon p has been chosen using the Akaike (AIC) criterion. The first step of the algorithm consists in estimating a VARX model of length p which describes the data. It can be shown that if $\hat{p}$ is the minimizer of the AIC criterion, $p = M\hat{p}$ with $M > 1$ is a possible choice. The AIC criterion reaches the minimum at $\hat{p} = 7$. For $M = 2$ this would lead to an order selection rule $p = 2\hat{p} = 14$. It turns out, however, that while this choice meets some asymptotic criterions it is not necessarily the best choice for finite data length N We have indeed verified in our experiments that $p = 9$ or $p = 10$ seem to provide the best results while also reducing the computational complexity (w.r.t. the choice $p = 14$).

As far as the choice of f, it only makes sense to consider $f \leq p$. We have adopted a validation based approach to the choice of f. Values of $f \geq 3$ have been tested and $f \geq 7$ seemed to provide the best results in terms of simulation error on validation data (without major differences between $f = 7$, $f = 8$ and $f = 9$.); thus $f = 7$ has been used.

Several models, with orders ranging in the interval $n \in [60, 140]$, have been estimated. Also the identification experiments have been repeated with two different levels of input injection with standard deviations 0.04 and 0.07 (the white noise signal $\mathbf{d}$ in Figure 2).

All identified models have been validated, according to the validation measure:

$$J = \frac{1}{\bar{N}} \sum_{t=1}^{\bar{N}} \mathrm{Tr}\left[\left(y_s(t) - y(t)\right) \left(y_s(t) - y(t)\right)^\top \right] \tag{3}$$

where y_s is the simulated output using the identified model while y is the output from the real plant.

The validation experiments have been carried out using three different levels of input excitation, namely with standard deviation 0.07, 0.04 and 0.016 (see figure 3). All experiments (identification and validation) have been carried out with a sampling frequency of $200Hz$.

As anticipated in Section IV, it is a standard practice in AO systems to model the input-output behavior using a static gain (Interaction Matrix, IM) computed as discussed

[2]Short for Vector AutoRegressive with eXogenous inputs.

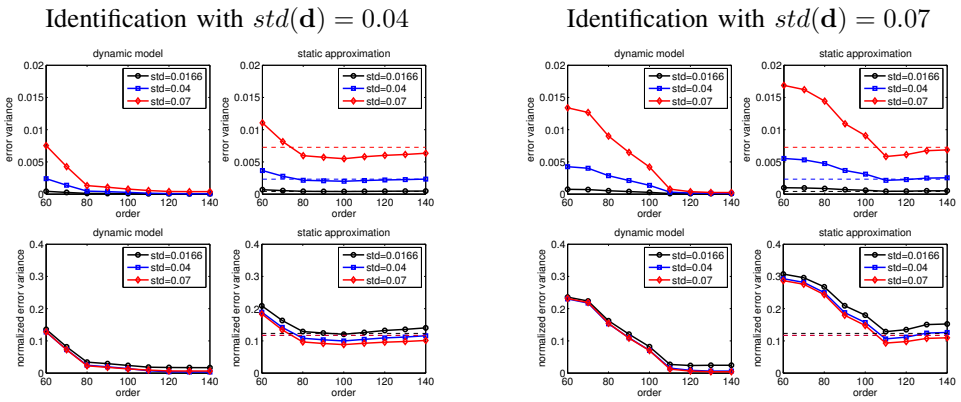

Fig. 3. Validation results (simulation error). Left hand side: using the identified model. Right hand side: using the static approximation (DC gain) and the IM (horizontal line). The injected noise $\mathbf{d}$ used in the identification step has standard deviation 0.04 (left) and 0.07 (right). The three curves refer to validation data with different level of injected disturbance $\mathbf{d}$ (0.07, 0.04, 0.016 respectively).

in Section IV. This is justified by the fact that, according to the discussion in Section III, the system should be well approximated by a constant gain (and a delay) in the frequency range of interest. The results of this paper seem to suggest that this is not the case; in fact the dynamic model does significantly improve in terms of simulation error.

In our validation experiments we therefore compare the validation results using: (i) the dynamic model we have identified, (ii) the standard static model, i.e. the IM computed using standard techniques (iii) the static approximation of the identified model, i.e. its DC gain, and (iv) a reduced order model of order n_r using the procedure discussed in Section V-B; the results are reported for an identified model of order $n = 100$ obtained using input excitation $\mathbf{d}$ of standard deviation 0.04. This choice was motivated by the fact that its static gain gives the best validation results among all static approximations, see Figure 3, the plot of the static approximation for identification with standard deviation 0.04[3].

The validation results can be summarized as follows:

a) The dynamic model outperforms the static model in essentially all situations. In fact the validation results show that an appropriate dynamical model performs about 40 times better (in terms of normalized error variance) w.r.t. the static model; this may suggest that a control design which uses the dynamic model may compare favorably with standard techniques based on static linear approximations (using the IM).

b) A reduced order model of order n_r (obtained using the procedure in Section V-B) performs as good as the full order identified model provided $n_r \geq 60$. See Figure 4.[4]

These results are in line with the discussions in [28], [16] in that identifying a large order model and then performing model reduction is sometimes to be preferred to direct low order model identification.

This may be very useful for the purpose of control design. Note in fact that currently used PI controllers require a memory which has the same dimension as the input space, i.e. 60. Hence a model-based control scheme could be implemented with about the same order of complexity as the standard PI controller.

c) The static model obtained from the DC gain of the (dynamic) identified model is comparable w.r.t. the static model obtained using the standard approach for the computation of the IM.

d) The dynamic models identified with large input excitation (standard deviation 0.07) perform slightly worse than those with standard deviation 0.04; this suggests that, perhaps, non-linear effects come into play. Also larger order models are necessary to reach comparable performance. Compare, for instance, the plots on the bottom left corners on the left and right panel in Figure 3.

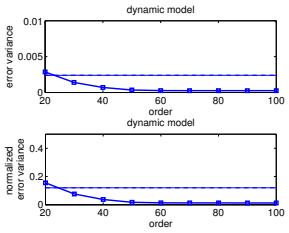

Fig. 4. Reduced order model (starting from identified model of order 100) v.s. Interaction Matrix.)

We have also analyzed the spectral content of the simulation errors $e_s(t) := y_s(t) - y(t)$ for both the simulation using the static and dynamic models. The signal $e_s(t)$ has 104 components (the number of sensed slopes); we have computed the power spectrum of its components. For reasons of space we report the power spectrum of the error only

[3]We have also validated reduced order models starting from different full order identified models (e.g. order 120 or 140) obtaining very similar results.

[4]Unfortunately we do not have any good physical insight as to why below $n_r = 60$ the performance degrades so rapidly while it is essentially unchanged for $n_r \geq 60$.

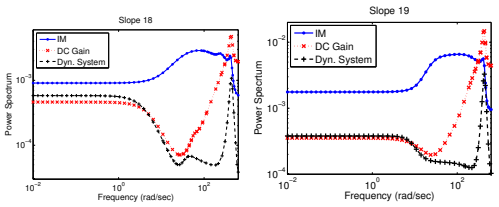

Fig. 5. Power spectrum of the simulation errors. Slope #18; fit: 87.17% (IM), 88.3% (DC Gain), 98.53% (Dyn. System). Slope #19; fit: 86.61% (IM), 85.67% (DC Gain), 98.18% (Dyn. System).

for two components; in particular we have selected the two slopes which yield, respectively, the maximum and minimum simulation error (normalized). It turns out the these are respectively slope #18 and #19 along the x axis.

Some representative results are reported in figure 5; it is clear that the frequency content of the error using the static models (both the IM computed using the standard tools in AO and the DC gain of the identified model) has a sharp peak in high frequency. It is also remarkable that, while the peak is still present using the dynamic model, its height and also its width are considerably reduced.

Note also that both the dynamic model and its static approximation (DC gain) perform better than the IM for low to medium frequency range.

It should also be stressed that these results have been obtained when the input is perturbed with a white noise process. Instead, during normal operating conditions, the "external excitation" is provided by the incoming turbulence. It is a well known fact that this perturbation has a "low-pass" spectrum [21], [10] and hence excites only the systems in the low to medium frequency range. It is therefore quite natural to expect that a dynamic model which performs better in that frequency range is to be preferred. Unfortunately, the data available does not allow to perform these sort of tests and, as mentioned in the introduction, we shall not be able to perform further test until the system will be operating in the Paranal observatory.

VII. Conclusions

In this paper we have reported our experience on the problem of modeling the "deterministic" part of an Adaptive Optics system. We have tackled the problem applying state-of-the-art subspace identification techniques to real data taken from a Multi-Conjugate Adaptive Optics Demonstrator developed at ESO. In order to be able to handle the large dimension of the data set we have developed a recursive version of the PBSID$_{opt}$ algorithm; the recursive version is interesting *per se* and, with minor modifications, can also be used to tackle identification of slowly time-varying systems.

The validation results are very encouraging, showing that the identified model outperforms currently used (static) models. We have also applied model reduction techniques, which have allowed to obtain reasonably sized models with very little loss in term of performance on validation data.

Future work will include exploring the possibility of using such models for the purpose of control design.

References

[1] U.M. Al-Saggaf and G.F. Franklin. On model reduction. In *Proc. of the 25th Conf. on Dec. and Cont.*, pages 1064–1369, Athens, Greece, 1986.

[2] R. Arsenault et al. MACAO-VLTI adaptive optics systems performance. *Proceedings of SPIE*, 5490:47–58, 2004.

[3] D. Bauer. Asymptotic properties of subspace estimators. *Automatica*, 41:359–376, 2005.

[4] X. Bombois, M. Gevers, and G. Scorletti. Open-loop versus closed-loop identification of Box-Jenkins models: A new variance analysis. In *Proc. 44th IEEE Conf. on Dec. & Control*, Seville, Spain, 2005.

[5] J.R. Bunch and C.R. Nielsen. Updating the Singular Value Decomposition. *Numer. Math.*, 31:111–129, 1978.

[6] A. Chiuso. On the relation between CCA and predictor-based subspace identification. *IEEE Trans. on Automatic Control*, 52(10):1795–1812, October 2007.

[7] A. Chiuso. The role of Vector AutoRegressive modeling in predictor based subspace identification. *Automatica*, 43(6):1034–1048, June 2007.

[8] A. Chiuso, R. Muradore, and E. Fedrigo. Adaptive optics systems: A challenge for closed loop subspace identifcation. In *Proc. of ACC*, 2007.

[9] P. Comon and G.H. Golub. Tracking a few extreme singualr values and vectors in signal processing. *Proceedings of the IEEE*, 78(8):1327–1338, 1990.

[10] J.M. Conan, G. Rousset, and P.Y. Madec. Wave-front temporal spectra in high-resolution imaging through turbulence. *J. Opt. Soc. Am. A*, 12(7):1559–1570, 1995.

[11] E. Fedrigo, M. Kasper, L. Ivanescu, and H. Bonnet. Real-time control of ESO adaptive optics systems. *Automatisierungstechnik*, 53(10):470–483, 2005.

[12] M. Gevers and L. Ljung. Optimal experiment design with respect to the intended model application. *Automatica*, 22:543–554, 1986.

[13] J.S. Gibson, C. Chang, and B.L. Ellerbroek. Adaptive optics: wavefront correction by use of adaptive filtering and control. *Applied Optics*, 39(16):2525–2538, 2000.

[14] G.H. Golub and C.R. Van Loan. *Matrix Computation*. The Johns Hopkins Univ. Press., 2nd ed. edition, 1989.

[15] K. Hinnen, M. Verhaeghen, and N. Doelman. A data-driven $\mathcal{H}_2$-optimal control approach for adaptive optics. *IEEE Trans. on Contr. Syst. Tech.*, 16(3):381–395, 2008.

[16] H. Hjalmarsson. From experiment design to closed-loop control. *Automatica*, 41(3):393–438, 2005.

[17] M. Kasper, E. Fedrigo, D. P. Looze, H. Bonnet, L. Ivanescu, and S. Oberti. Fast calibration of high-order adaptive optics systems. *J. Opt. Soc. Am. A*, 21(6):1004–1008, 2004.

[18] D.P. Looze. Minimum variance control structure for adaptive optics systems. *Journal of the Optical Society of America A*, 23(3):603–612, 2006.

[19] D.P. Looze, M. Kasper, S. Hippler, O. Beker, and R. Weiss. Optimal Compensation and Implementation for Adaptive Optics Systems. *Experimental Astronomy*, 15(2):67–88, 2003.

[20] E. Marchetti et al. On-sky testing of the multi-conjugate adaptive optics demonstrator. *The Messanger*, 129:8–13, 2007.

[21] R.J. Noll. Zernike polynomials and atmospheric turbulence. *JOSA*, 66(3):207–211, 1976.

[22] S. Oberti et al. Large DM AO systems: synthetic IM or calibration on sky? *Proceedings of SPIE*, 6272:627220, 2006.

[23] R.N. Paschall and D.J. Anderson. Linear quadratic Gaussian control of a deformable mirror adaptive optics system with time-delayed measurements. *Applied Optics*, 32(31/1), 1993.

[24] R. Ragazzoni, E. Marchetti, and G. Valente. Adaptive-optics corrections available for the whole sky. *Nature*, 403(6765):54–6, 2000.

[25] F. Roddier. *Adaptive Optics in Astronomy*. Cambridge University Press, 1999.

[26] M.C. Roggemann and B. Welsh. *Imaging through Turbulence*. CRC Press, 1996.

[27] T. Söderström and P. Stoica. *System Identification*. Prentice-Hall, 1989.

[28] F. Tjärnström. Variance analysis of L_2 model reduction when undermodeling: the output error case. *Automatica*, 39:1809 1815, 2003.

[29] Bin Yang. Projection approximation subspace tracking. *IEEE Transactions on Signal Processing*, 43(1):95–107, 1995.